

Narrowband Filter Considerations for LSST
C. Stubbs
April 30, 2015

Introduction

The baseline complement of LSST filters, *ugrizy*, is a slightly modified implementation of the SDSS passbands, augmented by a *y* band filter to take advantage of the enhanced CCD response in the 850-1000 nm regime. This filter set does a good job of both Galactic and extragalactic science, providing good photo-*z* estimates as well stellar characterization.

This document considers possible augmentations to this filter set, particularly narrower passbands. Scientific drivers for this include large scale structure studies using emission line galaxies in thin redshift shells, studying extragalactic star formation rates as a function of redshift and environment, mapping narrow line emission across the Milky Way, using planetary nebula luminosity function (PNLF) as a distance indicator, and improved stellar characterization in resolved stellar populations within the local group. The goal of this document is not to make this science case, but rather to explore these opportunities in the context of the technical limitations imposed by the LSST optics and camera system. Ivezić (2007) describes the merits of narrowband imaging for AGB star science. The Skymapper project has elected to use a split *u* band, in order to improve stellar metallicity determination (Keller et al 2008).

If we take the LSST sensor QE of 0.3 at $\lambda=1$ micron as setting the upper limit on usable narrowband wavelengths, this corresponds to H- α emission at a redshift of 0.52. Star formation rate scales (see Fig 3) as roughly $(1+z)^2$ out to $z \sim 1$, so we would expect the strength of H α emission at $z=0.52$ to be over two times higher than at the current epoch. Emission from the [OII] line at 372.7 nm at $z=1.68$ would also fall within this passband.

The H α +NII and [OIII] lines are blends, with separations of $3.5\text{nm}(1+z)$ and $4.8\text{nm}(1+z)$, respectively. These separations are considerably smaller than the narrowest passband of filters we can expect to obtain. This is a good thing.

Properties of the LSST Beam

The LSST at the filter location is a hollow cone of rays, with the (virtual) chief ray normal to the filter surface. The LSST filter is 150 mm from the focal plane, on axis. The $f/1.23$ annular beam footprint therefore has an outer diameter at the filter that spans about 18 cm. There is a 1:1 correlation between the ray angle and its radial position relative to the (virtual) chief ray at the center of the beam.

The angle of incidence on the filter ranges from 14 to 23 degrees, as measured from the normal to the filter surface, with the 23 degree rays striking the filter at the outer edge of the annular beam footprint.

Minimum Achievable Passband

Thin-film interference filters suffer an angle-of-incidence dependent shift in transmission properties, with passband edges shifting to bluer wavelengths by an amount approximated by $\lambda(\theta) = \lambda_o \sqrt{1 - ((\sin \theta) / n_{\text{eff}})^2}$, where n_{eff} is the effective index of refraction of the thin film layers and θ is the angle off normal. For many filters the effective index of refraction is polarization dependent and this is an additional source of passband broadening. Typical values of n_{eff} are in the range of 1.5 to 2.5.

Figure 1 shows the shift in wavelength expected for values of $n_{\text{eff}} = 1.8, 2.0$ and 2.2 , across the range of angles of incidence in the LSST beam.

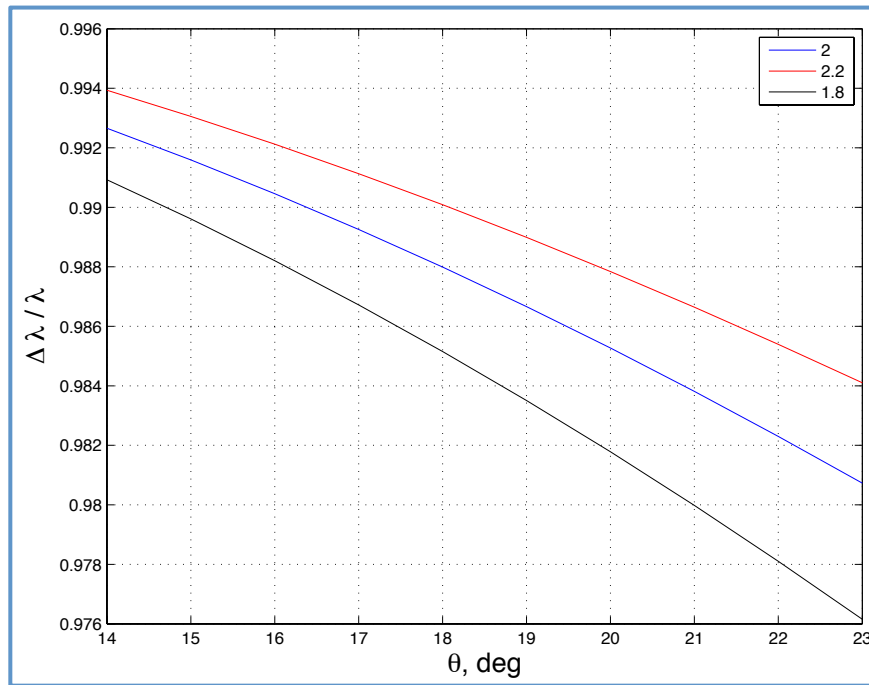


Figure 1. Incidence angle dependence of wavelength shift. The horizontal axis spans the range of angles of incidence in the LSST beam. The vertical axis shows the fractional change in wavelength, compared to $\theta=0$, for the effective index values of 1.8, 2.0 and 2.2.

For $n_{\text{eff}} = 1.8$, the edge-to-edge shift in wavelength change ranges from 0.976 to 0.991, a span of 1.5%. Note that these are not equally weighted, there are more photons impinging at 23 degrees than at 14 degrees. So a delta-function normal incidence filter produces a skewed, blue-shifted response in the LSST beam. For the longest wavelength narrowband filter we might imagine placing in the beam, centered at 1000 nm, this limits our bandwidth to 15 nm, convolved with the normal-incidence response function of the filter. At 500 nm the angle-driven convolution width is half this value, about 7.5 nm. Note that we have ignored any possible polarization dependence. If we fabricate filters with higher

effective indices, the effect is attenuated. At $n_{\text{eff}}=2.2$ the fractional broadening is $(0.944 - 0.984)=1\%$, which corresponds to 5 nm at our midpoint wavelength of 500 nm.

Given the size and shape of the LSST filters, it is probably impractical to imagine producing a filter with a uniform normal-incidence width of under 10 nm. With a high-index thin film narrowband interference filter, we can probably expect to achieve a transmission FWHM of 15-20 nm in the LSST beam. We'll adopt 20nm as a conservative canonical value for what follows. This is about a factor of 7 narrower than the typical LSST broad passband.

Signal Strength for Emission Line Objects

For a 20 nm wide filter, an emission line object would appear brighter than the continuum expectation by an amount $\Delta m = -2.5 \log((EW+20)/20)$, where EW is the observer frame emission line equivalent width in nm. This relationship is shown in Figure 2. For galaxies with broadband and narrowband photometric uncertainties each of 0.05 mag, leading to an uncertainty in narrowband vs. broadband difference Δm of 0.07 mag, we would have a 3σ EW flux-excess threshold of 0.21 magnitudes, which in turn requires an (H α +NII) equivalent width in excess of 4 nm, or 40 Å.

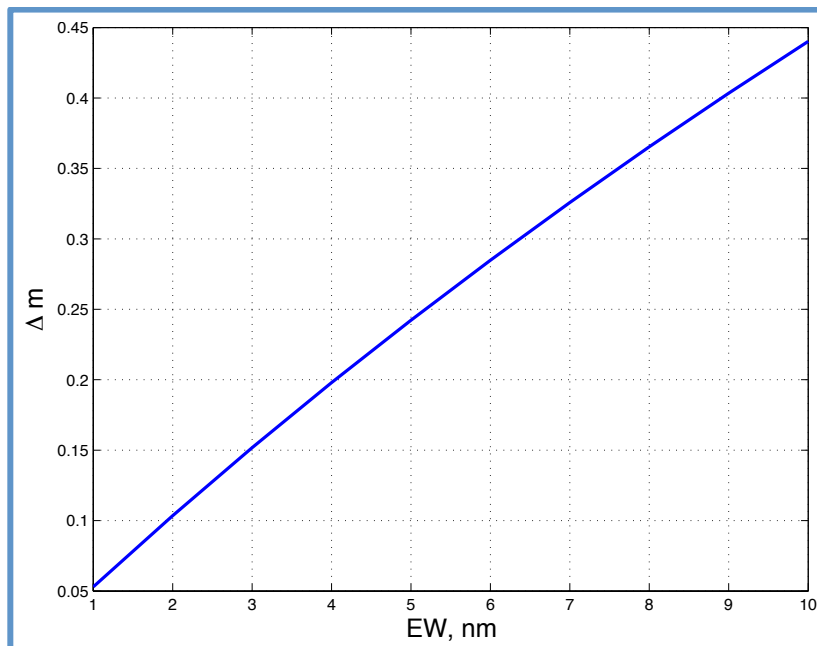


Figure 2. Magnitude excess relative to continuum expectation as a function of emission line equivalent width. This is for a 20 nm FWHM filter.

How does $EW=40\text{\AA}$ compare to typical observed values? Figure 3 is reproduced from a study of emission line EW values vs. galaxy mass and redshift, by Fumagalli et al (2012). Their results show a redshift dependence of $EW \sim (1+z)^{1.8}$. For $0.2 < z < 0.4$, about half the low mass galaxies exceed our nominal 3σ threshold for $SNR > 20$ observations, which is shown as the red horizontal line that cuts across the top 3 panels in Figure 3.

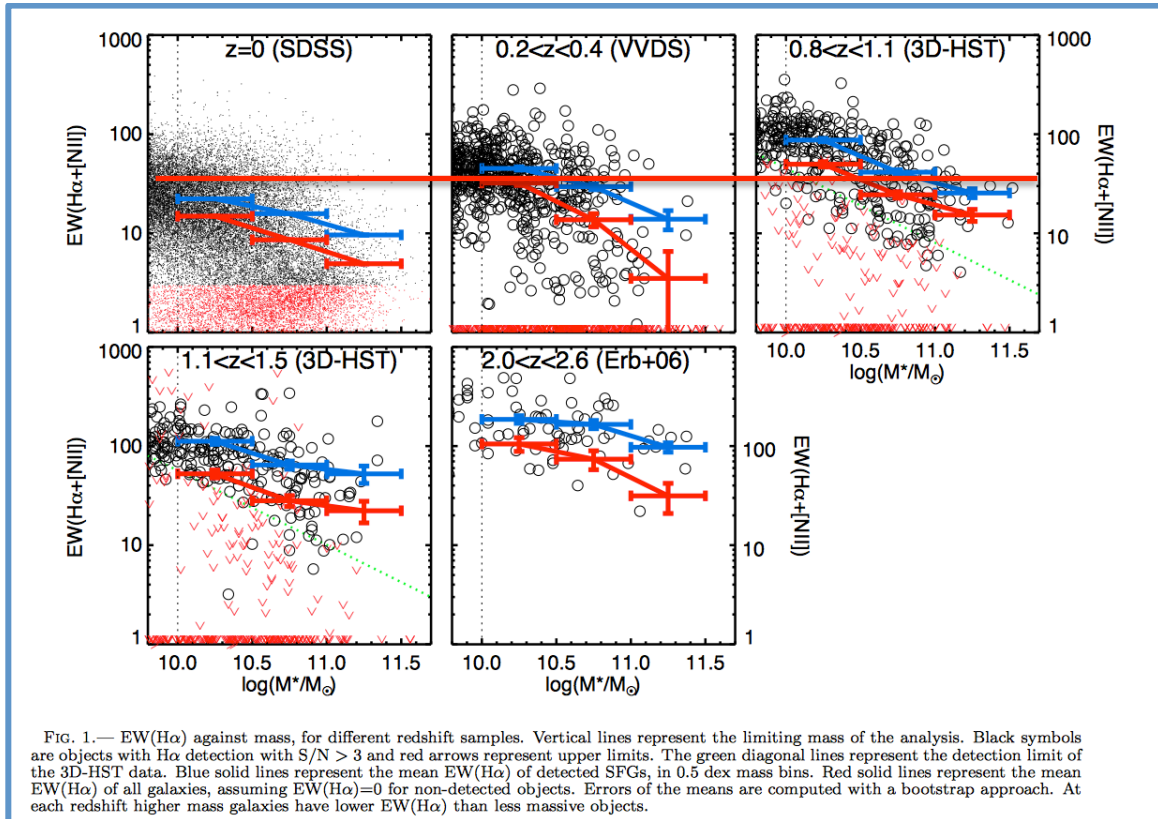


Figure 3. Emission line strength ($H\alpha + NII$) vs. redshift and galaxy mass. Our 3σ detection threshold of 40\AA for $\sigma_m=0.05\text{ mag}$ in both the y band and narrowband filter, for a 20 nm FWHM filter, is shown as the red horizontal line. At $z \sim 0.5$ we would expect to detect about half of the emission line objects shown in this figure. Figure reproduced from Fumagalli et al (2012). The LSST CCDs aren't sensitive to $H\alpha$ at redshifts beyond about 0.52.

We can conclude from this that an $H\alpha$ filter tuned to a redshift of 0.5 should pick up about half the sources shown in Figure 3, if we achieve $SNR > 20$ in both the narrowband and broadband fluxes. I think this also means it will likely be more difficult to detect $[OII]$ at 3727 since the EW of this feature is typically weaker than the $H\alpha$ line.

Large Scale Structure Applications

How thick is the line-of-sight redshift shell? For a 20nm filter width centered on $(1+z)*656.3\text{ nm} = (1.52)*656.3 = 997\text{ nm}$, with a width of 20 nm . We would know that

(apart from contamination by non H α objects) each emission line source resides in a rather flat-topped redshift bin that spans from 987 to 1007 nm, so that $0.503 < z < 0.534$. We can compare this to the per-galaxy photometric redshift uncertainties we expect from the LSST broadband photometry alone. The LSST web site points to a photo-z calibration paper (<http://www.lsst.org/files/docs/Phot-z-plan.pdf>) that stipulates for SNR=30 (higher than the SNR=20 we assumed above for the narrowband photometric magnitudes) the per-object photo-z uncertainty is expected to be $dz = 0.05 (1+z)$. We'll assume this is a 1σ Gaussian-equivalent, so that 68% of the objects should have photo-z estimators that lie within $dz=0.1(1+z)$ of their true value.

The comparable redshift uncertainty for an SNR=20 (H α +NII) emission line object that lands within our 20 nm passband is $dz=0.02 (1+z)$, a fivefold improvement but of course only over a very limited redshift range.

How thick is this emission line object redshift shell in Megaparsecs and how does that compare to the BAO correlation length of ~ 100 Mpc? The redshift limits of $z=0.503$ and 0.534 correspond to angular diameter distances of 1.277 Gpc and 1.318 Gpc, respectively. So the redshift shell thickness spans an angular diameter distance difference of 41 Mpc. If we instead take luminosity distances we obtain a thickness of $3.101 - 2.884 = 217$ Mpc. I'm actually not sure which of these (if either) is the most appropriate... but in either case we can probe correlation statistics with a galaxy population that has biasing different from the LRG's used for spectroscopic BAO surveys. We also ought to be able to measure the angular diameter distance to this redshift using transverse BAO statistics, after properly correcting for the finite shell thickness.

Other Narrowband Science Opportunities Table I lists a few, but by no means all, other possibilities for narrowband filters. In some cases we can select filters that have discrimination capabilities for individual stars in the local group, that also provide interesting extragalactic emission line objects within the same passband.

Table I. Potential Narrowband Filter Choices and Applications.

Central wavelength (Å)	Galactic structure and stars	Ly- α 1215Å redshift (quasars)	H α +NII 6563/6548/6583Å redshift (large scale structure)	[OIII] 4959/5007Å redshift (PNLF distances)
3900	Stellar metallicity	2.2	NA	NA
5007	PNe, SN remnants	3.1	NA	To 50 Mpc, typically
7780	Stellar TiO	5.4	0.18	NA
8210	Stellar CN	5.7	0.25	NA
6563	H- α map	4.4	0.0	NA
10000	L dwarf classification	7.2	0.53	NA

Exposure Time Implications

A 20 nm wide filter has about a sevenfold reduction in throughput, compared to typical LSST filters. So to achieve the same source flux would require seven times the exposure time as the broadband exposure. Picking narrowband spectral regions in the NIR with OH emission below the broadband average would reduce this somewhat. Figure 4 shows the anticipated LSST quantum efficiency curves for the two candidate sensor vendors.

A concrete example of an additional-filter survey would be the Skymapper “v” band at 390 nm, with a passband of about 30 nm FWHM. Reaching the single-epoch depth equivalent to the LSST *ugrizy* bands would require an exposure time of 60 seconds, but we could accomplish this with better shutter-open efficiency by taking a pair of 30 second exposures at each pointing. For 18,000 square degrees at 9.6 square degrees per field, this is 1875 pointings. Allowing for overlaps we’ll round this up to 2000, which will require 33 hours of integration, which could easily be done in fewer than 10 nights of dark-time survey operation. To span the full range of RA’s we’d have to distribute this through the year, however.

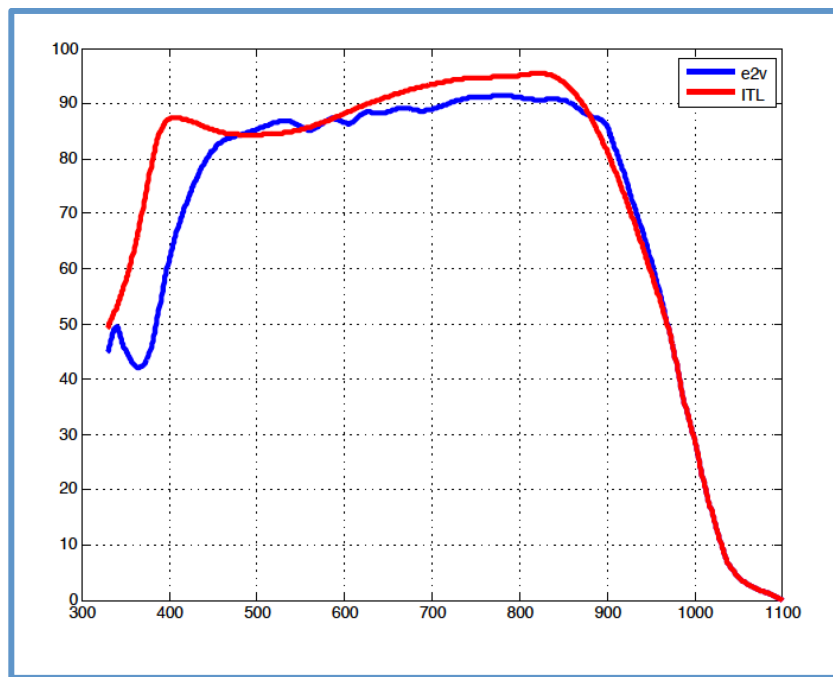


Figure 4. LSST sensor QE curves for the two candidate vendors.

References

Ivezic, Z. The Impact of LSST on Asymptotic Giant Branch Star Research, ASP Conference Series, **378**, p 485, F. Kerschbaum, C. Charbonnel, R.F. Wing, eds, (2007).

<http://www.astro.washington.edu/users/ivezic/Publications/AGB2007.pdf>

Abell, P. *et al.*, LSST Science Book v. 2

Best, P. *et al.*, HiZELS: the High Redshift Emission Line Survey with UKIRT, arXiv 1003.5183 (2010).

Keller, S. *et al.*, The Skymapper Telescope and the Southern Sky Survey, Publications of the Astronomical Society of Australia **24** (1) (2008).

Fumagalli, M. *et al.*, H α EQUIVALENT WIDTHS FROM THE 3D-HST SURVEY: EVOLUTION WITH REDSHIFT AND DEPENDENCE ON STELLAR MASS, arXiv:1206.2645v2 (2012).